PHILOSOPHICAL TRANSACTIONS OF THE ROYAL SOCIETY B BIOLOGICAL SCIENCES

Efficiency and Evolution of Water Transport Systems in Higher Plants: A Modelling Approach. II. Stelar Evolution

A. Roth, V. Mosbrugger and H. J. Neugebauer

Phil. Trans. R. Soc. Lond. B 1994 **345**, 153-162
doi: 10.1098/rstb.1994.0094

Efficiency and evolution of water transport systems in higher plants: a modelling approach. II. Stelar evolution

A. ROTH[1], V. MOSBRUGGER[1] AND H. J. NEUGEBAUER[2]

[1]*Institut und Museum für Geologie und Paläontologie der Universität Tübingen, Sigwartstr. 10, D-72076, Tübingen, Germany*
[2]*Institut für Geodynamik, Universität Bonn, Nußallee 8, D-53115, Bonn, Germany*

SUMMARY

Different stelar arrangements have developed through evolution of land plants. The first stele to appear was a central strand (protostele) consisting of tracheids or hydroid-like cells. In more derived steles (e.g. actinostele, siphonostele), a location of the conducting elements at relatively more peripheral regions of the axis can be observed. It has been shown that the trend in stelar evolution in early land plants from protostele to actinostele or siphonostele has little to do with an increase of the flexural stiffness in the axis. Hence, it is to be expected, that the (early) stelar evolution reflects an optimization process of the water conducting capabilities of the stem. To test this hypothesis, the effectiveness of protostele and siphonostele in water conduction was analysed numerically. The results demonstrate that the hydrodynamic behaviour of a plant axis depends not only on the relative amount of its conducting tissues, but also on the arrangement of the xylem within an axis. A protostele and a siphonostele with identical distance between outer xylem boundary and site of transpiration may, therefore, be identical with regard to water transport efficiency.

1. INTRODUCTION

The term 'stele' describes the entire conducting tissues of a primary plant axis and represents the architectural arrangement of the conducting bundles. It is restricted to the primary state of a plant and should not be used for that vascular tissue which is produced by secondary growth (Beck *et al.* 1982). Several stelar constructions appeared during evolution of the land plants (see, for example, Bold *et al.* 1980). The most primitive type consists of one central strand only and is denoted as the protostele. It is a characteristic feature of the earliest land plants, such as *Cooksonia* or *Rhynia*, which were composed of leafless axes (telomes) (Edwards & Fanning 1985). The protostele underwent subsequential developmental changes when complexity of the entire axis increased during evolution of higher land plants (Stewart & Rothwell 1993). Enlarging of the outer surface of the stele by sending protuberances into the adjacent parenchyma formed the actinostele. In the next step, the conducting tissue was arranged as a hollow cylinder with an internal pith of parenchyma, a construction termed the siphonostele. The steles described so far can be found today in several recent plant groups. *Psilotum nudum*, for example, shows a protostele or actinostele and the ferns as a whole express a great variety of stelar constructions even in the same individual. Further evolutionary changes of the stele led to the distribution of the conducting units over the entire cross-sectional area, resulting in the stelar constructions eustele and atactostele which are characteristic for the modern plant groups of dicotyledons and monocotyledons. Thus, the evolution of the stele shows a tendency to shift the conduits to the peripheral region with a final stage of dividing the conducting area into subunits.

Several theories are dealing with the details of evolutionary sequence of the different stelar arrangements. According to Zimmermann (1959), for example, all cormophytic organs are the result of conceptual simple processes, such as overtopping or fusion of elementary plant axes or telomes. A eustele, for instance, would on this view be a product of fusion of protostelar telomes. Beck *et al.* (1982), however, pointed out that a gymnospermic eustele was formed by longitudinal dissection of an original actinostele. Whatever evolutionary development occurred, the changes of stelar architecture were coupled with increasing diameter and height of the axis, as was found by Niklas (1984). Additionally, a good correlation between the deviation from the protostelar concept and stratigraphy is evident, as younger taxa developed the tendency of more complex stelar arrangements. According to Bower (1908, 1935), plants tend to maintain a constant ratio of xylem surface to xylem volume when increasing in size (ontogenetically and phylogenetically). On an ontogenetic level, this was demonstrated for *Psilotum nudum* by Bierhorst (1971). Thus, the evolutionary development of the plant axis should be linked with the evolution of the stelar architecture. Niklas (1984,

Phil. Trans. R. Soc. Lond. B (1994) **345**, 153–162
Printed in Great Britain

1992), however, demonstrated that the ratio of xylem surface to xylem volume may increase or decrease in early land plant evolution and he pointed out that this value is influenced primarily by creating hydraulic interconnections between the various parts (leaves and stem) of a more complex plant body. Apart from these studies, the evolution of the stele was regarded as being related to the increasing mechanical demand of the axis due to the fact that the lignified xylem represents an important stabilizing factor for plants (see, for example, Zimmermann 1959). A peripheral position has a strengthening effect by increasing bending stiffness. This improvement of stability is not only important when the self weight (statical load) of the axis itself increases, but also with respect to the bending forces imposed by the wind, which has to be regarded as the dominating mechanical load acting on upright plant axes (Vincent & Jeronimidis 1991). The mechanical properties of the stelar constructions of numerous fossil and recent taxa were investigated by Speck & Vogellehner (1988). They found that the mechanical effectiveness of the early constructions protostele, actinostele and siphonostele are not essentially different. An improved stability was achieved by later steles, such as the eustele. Moreover, early land plants often showed a hypodermal sterome which was more important for the stability of the plant (Speck 1991). Thus, the evolution of the stele was obviously caused not only by mechanical factors.

In the present paper, we return in some respects to the basic idea of Bower by assuming that water transport is an important factor in stelar evolution. The water transport properties of two different stelar types, the protostele and the siphonostele, were investigated by performing computer simulations describing the hydrodynamic behaviour of the steles in order to compare their water transport efficiency.

2. THE MODEL SYSTEM

The mathematical model, which was used for the numerical simulations, is composed of two coupled differential equations describing the behaviour of a poroelastic system consisting of two phases, porous material matrix and fluid within the void spaces. The model was introduced in a previous paper (Roth *et al.* 1994), but a brief explanation of the underlying principles will be given here. The mechanical behaviour of the material matrix is described by Hooke's law in its general form, while the fluid moves within the material matrix according to the law of Darcy which defines the relative velocity of the fluid flow as being dependent on the pressure gradient and the hydraulic conductivity. Both equations concerning material matrix and fluid are coupled in order to calculate the behaviour of the entire two-phases system. Any mechanical load, for instance, will cause fluid flow because of deformations of the fluid-filled material matrix whereas changes of the fluid content will cause deformations of the material matrix. The differential equations are solved with the Finite Element method (FEM), by which the considered area is substituted by a grid consisting of a set of discrete elements. The elements are defined by nodes. The system of equations is solved for each element and the behaviour of the entire grid is directed by the behaviour of its subareas (Zienkiewicz 1989). This numerical method permits the consideration of arbitrary grids and of areas which are composed of many different materials. This is achieved by combining the elements with appropriate physical parameters which define the material properties of an element. The corresponding computer program NAPE (Wallner 1990) allows for the calculation of axisymmetric grids. Mathematical model and program were originally formulated in order to simulate porous rock compaction (Grün *et al.* 1989). The parameters which were used for simulating the behaviour of plant tissues will be introduced in the next section together with the model structures. The boundary conditions which define the existence of free and fixed boundaries and the external loads will be explained in the next section. The unknown parameters are node displacements in the horizontal and

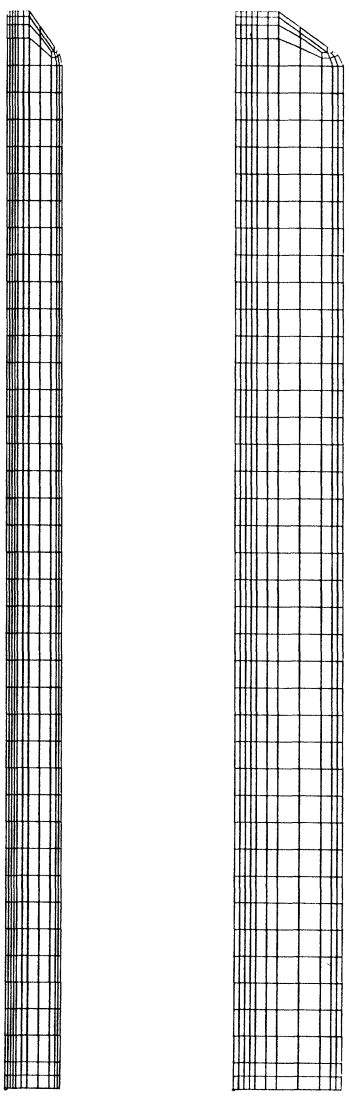

Figure 1. The two different grids which were used for the model simulations. The dimensions are: left, radius = 0.5 mm, height = 10 mm; right, radius = 1.0 mm, height = 10 mm.

PHILOSOPHICAL TRANSACTIONS OF THE ROYAL SOCIETY B BIOLOGICAL SCIENCES

Table 1. *The listing of all model calculations*
(The transpiration rate amounted to 5×10^{-6} mm^3 mm^{-2} s^{-1} in all cases.)

structure	stelar type	radius of axis/mm	area of xylem/mm^2 (cross-sectional)	ratio of xylem area to total area	distance of xylem to surface/mm	steady state reached after/s
P1	protostele	0.5	0.0020	0.0025	0.475	300
P2	protostele	0.5	0.0079	0.0100	0.450	100
P3	protostele	0.5	0.0310	0.0400	0.400	35
P4	protostele	0.5	0.0710	0.0900	0.350	18
P5	protostele	1.0	0.0079	0.0025	0.950	500
P6	protostele	1.0	0.0310	0.0100	0.900	250
P7	protostele	1.0	0.1260	0.0400	0.800	120
P8	protostele	1.0	0.2800	0.0900	0.700	70
S1	siphonostele	0.5	0.0059	0.0075	0.450	130
S2	siphonostele	0.5	0.0137	0.0170	0.400	70
S3	siphonostele	0.5	0.0393	0.0500	0.350	30
S4	siphonostele	0.5	0.0550	0.0700	0.300	16
S5	siphonostele	1.0	0.0236	0.0075	0.900	250
S6	siphonostele	1.0	0.0550	0.0170	0.800	150
S7	siphonostele	1.0	0.1570	0.0500	0.700	70
S8	siphonostele	1.0	0.2200	0.0700	0.400	39
S9	siphonostele	1.0	0.4320	0.1380	0.600	35
S10	siphonostele	1.0	0.3770	0.1200	0.600	35
S11	siphonostele	1.0	0.2750	0.0875	0.700	70
S12	siphonostele	1.0	0.2500	0.0800	0.700	74
S13	siphonostele	1.0	0.2120	0.0675	0.700	74
S14	siphonostele	0.5	0.0530	0.0675	0.350	20

Table 2. The material parameters for parenchyma and xylem.

parameter	parenchyma	xylem	references
E-modulus/kPa	5×10^4	5×10^6	Burström *et al.* (1970); Niklas (1988); Jeronimidis (1980); Vincent (1982)
Poisson-ratio	0.25	0.25	Chappell & Hamann (1968); Wainwright *et al.* (1976)
hydraulic conductivity/ (mm^2 s^{-1} kPa^{-1})	1×10^{-6}	1×10^{-2} (longitudinal) 1×10^{-4} (horizontal)	Raven (1984)
compressibility of grain/ (kPa^{-1})	1×10^{-6}	1×10^{-7}	estimated
porosity	0.3	0.7	estimated
compressibility of fluid/ (kPa^{-1})	5×10^{-7}	5×10^{-7}	Weast & Astle (1983)

vertical direction, u_x and u_y, and fluid pressure p which is calculated as difference to the initial value $p_0 = 0$. In the following sections, p will be termed as fluid pressure or hydrostatic pressure, but formally it represents always the difference to the initial value.

3. THE MODEL STRUCTURES

Two different grids where created which represented simple leafless axes (or telomes) of early land plants. They show different radius-to-height proportions and are depicted in figure 1. It should be mentioned, that the grids are halfspaces with the axis of rotation at the left. The radius amounted to 0.5 and 1.0 mm and the height amounted always to 10 mm. The model plants were equipped with a protostele or siphonostele of different sizes by combining the respective elements building up the stele with the appropriate material parameters. The rest of elements were related to parenchyma. All variations of structures are summarized in table 1, while the physical parameters defining xylem or parenchyma are given in table 2 together with their references. The dimensions of the model axes and the 'xylem' structure correspond to values found in early land plants. *Cooksonia* and *Rhynia*, for example, may have a stem radius of 0.5 or 1.0 mm. The xylem area of their protosteles are also within the ranges chosen for the model structures (e.g. cross sectional area of xylem of P3 = 0.031 mm^2, cross sectional area of xylem of *Cooksonia pertonii* = 0.041

PHILOSOPHICAL TRANSACTIONS OF THE ROYAL SOCIETY B BIOLOGICAL SCIENCES

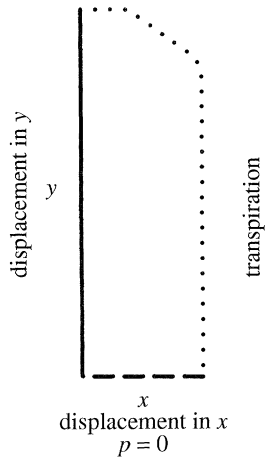

Figure 2. Boundary conditions of the model axes. The nodes at the axis of rotation (left axis) are allowed to move vertically, whereas the nodes at the bottom (= dashed line) may perform horizontal displacements. The fluid outflow (= transpiration) occurs over the surface which is represented by a dotted line.

mm^2 (Niklas 1984)). The material parameters used for the simulation are discussed in a previous paper (Roth *et al.* 1994). The boundary conditions define the behaviour of the boundary nodes of the grid and are shown in figure 2. All external factors will act upon these peripheral nodes (for a mathematical description of the boundary conditions see Bear 1979). Two boundary conditions were applied in the model.

The Dirichlet boundary conditions define the solutions of the unknown quantities for the boundary nodes, here displacement and fluid pressure. The nodes of the rotational axis (= *Y*-axis) are allowed to move vertically only and the nodes of the bottom (= *X*-axis) can perform displacements in the horizontal direction only. In this way, the structure is fixed in space. Additionally, the bottom serves as a free boundary referring to the fluid pressure by defining $p_{start} = 0$ as constant with time for the bottom nodes. This arrangement simulates a fluid reservoir below the bottom and a free water inflow into the axes. This means, that the model plants were saturated with water during the calculations. A root system was not included in the model structures.

The Cauchy boundary conditions describe an external load acting on the considered system via the boundary area and include parameters such as mechanical force or rates of fluid flow into or out of the system. In simple terms, these boundary conditions define an 'interface' between structure and environment. Therefore, Cauchy boundary conditions allow for simulation of transpiration by defining a rate of outflow per element. A transpiration rate of 5×10^{-6} mm^3 mm^{-2} s^{-1}, which is a typical value found in higher plants, was assumed (Altman & Dittmer 1973). Thus, the outer surface of the structures was simulated by the rate of outflow only.

The calculations are performed until the steady state condition was reached. In this state, inflow equals outflow and the calculated values are constant with time.

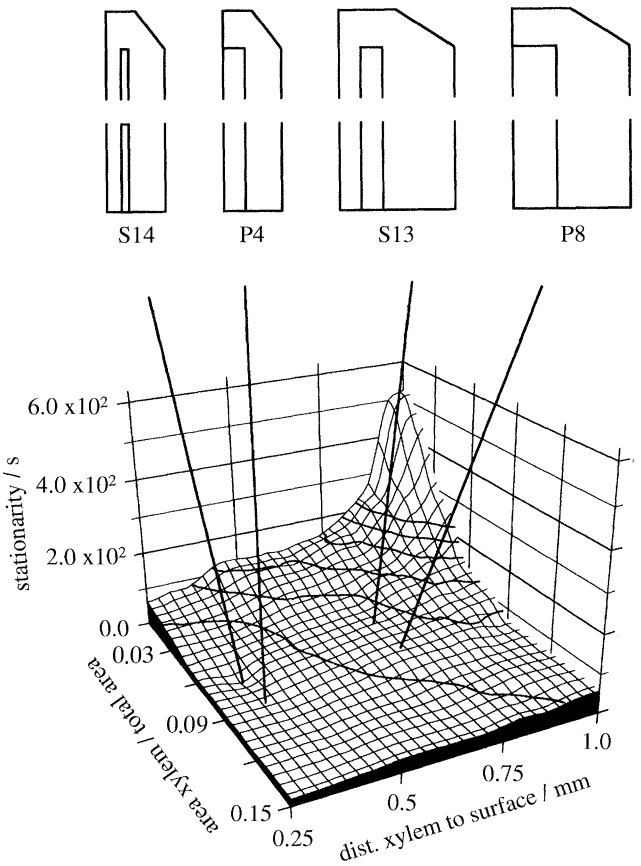

Figure 3. Time spans which are required by the different model structures to attain the steady state, plotted against *DX* (distance between outer xylem boundary and surface) and *RX* (ratio of cross-sectional area of xylem to entire cross-sectional area) in a three-dimensional representation. Four concrete structures (P4, P8, S13 and S14, see table 1) pointing to their data are integrated in the graph. Only the top and the bottom of the structures are drawn.

4. RESULTS

(*a*) *Temporal behaviour*

After starting the calculation, the initial pressure field changes due to the outflow. The resulting gradient of pressure leads to a fluid inflow from the bottom. During the time period of non-steady state, a loss of fluid occurs. When stationarity is attained, inflow equals outflow. The time span T_{stat} which is required to reach the steady state is therefore an indication of efficiency. The temporal behaviour showed to be depending on two quantities: the ratio of cross-sectional area of xylem to entire cross-sectional area (*RX*, defines relative conducting area) and the distance between the outer xylem boundary and surface (*DX*). In a three-dimensional representation, T_{stat} is plotted against *RX* and *DX* (figure 3). The corresponding values are listed in table 1. Four concrete halfspaces are included in the graph in order to permit a direct comparison between different structures. The halfspaces with identical stelar type (P4 and P8, S13 and S14) are equal with reference to *RX*, whereas the structures with equal radius (P4 and S14, P8 and S13) show identical *DX*. Only the lower

PHILOSOPHICAL TRANSACTIONS OF THE ROYAL SOCIETY B BIOLOGICAL SCIENCES

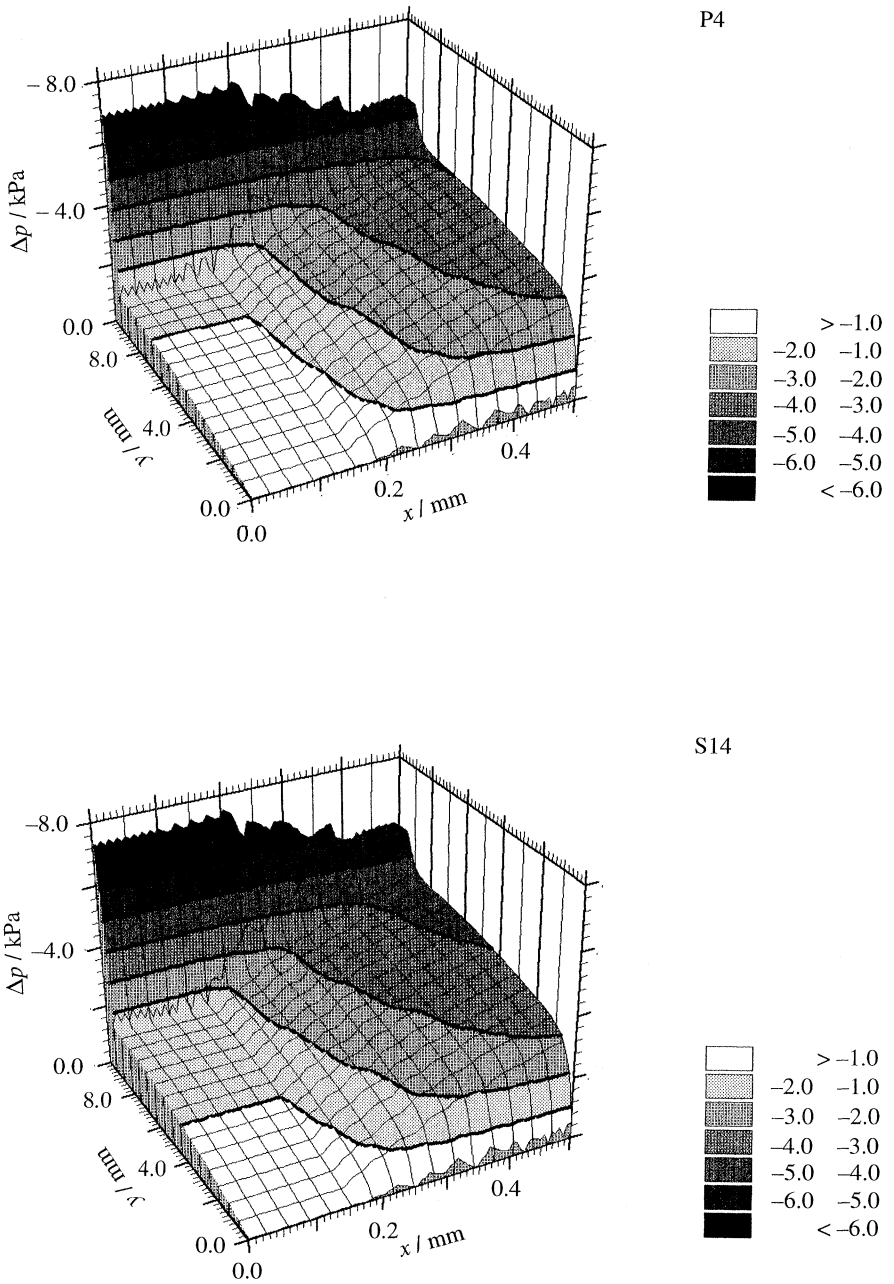

Figure 4. Pressure fields of the structures P4 and S14 at the steady state. The contour lines are equidistant starting with the least negative pressure values.

part and the upper part of the structures are shown. The graph clearly shows the temporal behaviour to be dependent on *RX* and *DX*. Combination of high *DX* and low *RX* results in a strong increase of T_{stat} which is influenced, therefore, not only by the relative amount of conducting tissue supplying a given plant axis, but also by the arrangements of the conduits. As a consequence, a siphonostele is able to reach the steady state as fast as a protostele with the same *DX*. This is demonstrated clearly by the four example structures included in the figure.

(*b*) *Fluid pressure field and fluxes*

The pressure fields of the four structures included in figure 3 are depicted in figure 4 (P4 and S14) and figure 5 (P8 and S13). The structures are in the steady state. In these graphs, the values of excess fluid pressure at the time of equilibrium ($= T_{stat}$) are plotted against the *X*- and *Y*-coordinates of the axes. The structures with radius = 1.0 mm (P8 and S13) show much steeper horizontal gradients of fluid pressure, when compared with P4 and S14 (radius = 0.5 mm). This is due to the different thickness of the parenchymatic layer separating stele and surface. The fluid pressure values of the structures with same *DX* (P4 and S14, P8 and S13) are almost identical. Obviously, structures with protostele or siphonostele, but with equal dimensions and equal distance between conduits and transpiring surface may show almost identical pressure fields. Furthermore, the resulting pressure values show that an axis

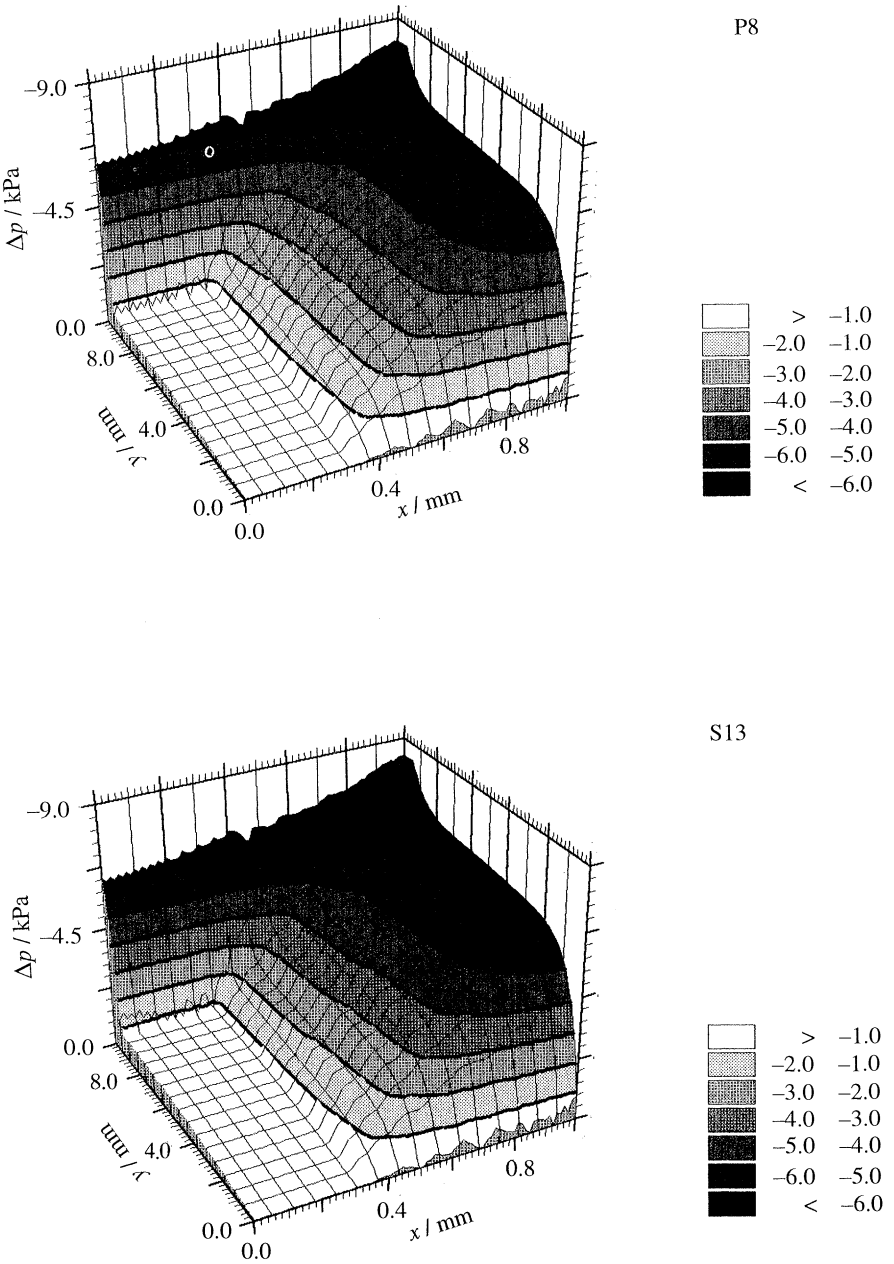

Figure 5. Pressure fields of the structures P8 and S13 at the steady state. The contour lines are equidistant starting with the least negative pressure values.

with protostele cannot be distinguished from a siphonostele of the same total radius (P4 and S14, P8 and S13) by comparing their fluid pressure fields, as the pith is isolated by the surrounding siphonostele and develops the same pressure values. This phenomenon was also found by Molz & Boyer (1978) while calculating the distribution of water potentials in a growing apex.

The different conducting areas of both stelar types are compensated by higher fluid velocities occurring in the siphonosteles. This is shown by the longitudinal component of fluid velocity, v_y. In figure 6, this parameter is plotted against X- and Y-coordinates for structures P8 and S13, both in equilibrium. The higher fluid velocities occurring in the siphonostele are caused by a correspondingly steeper pressure gradient in the longitudinal direction. This is evident when the fluid pressure values of the steles shown in figure 5 are compared.

The induced fluxes occurring in P8 and S13 at different times are shown as flow vectors in figure 7 (P8) and figure 8 (S13). Only the lower part ($Y = 0$–3 mm) and the upper part ($Y = 7$–10 mm) are represented. The length of a vector is related to the vector of the highest total velocity which has a fixed maximal length. Highest velocities occur, as expected, in the stele. The flow velocity fields of protostele and siphonostele are also different with respect to their temporal development. The directions of flow of structure P8 does not change with time. Here, a longitudinal flow runs through the stele with horizontal fluxes branching off. A temporal development is

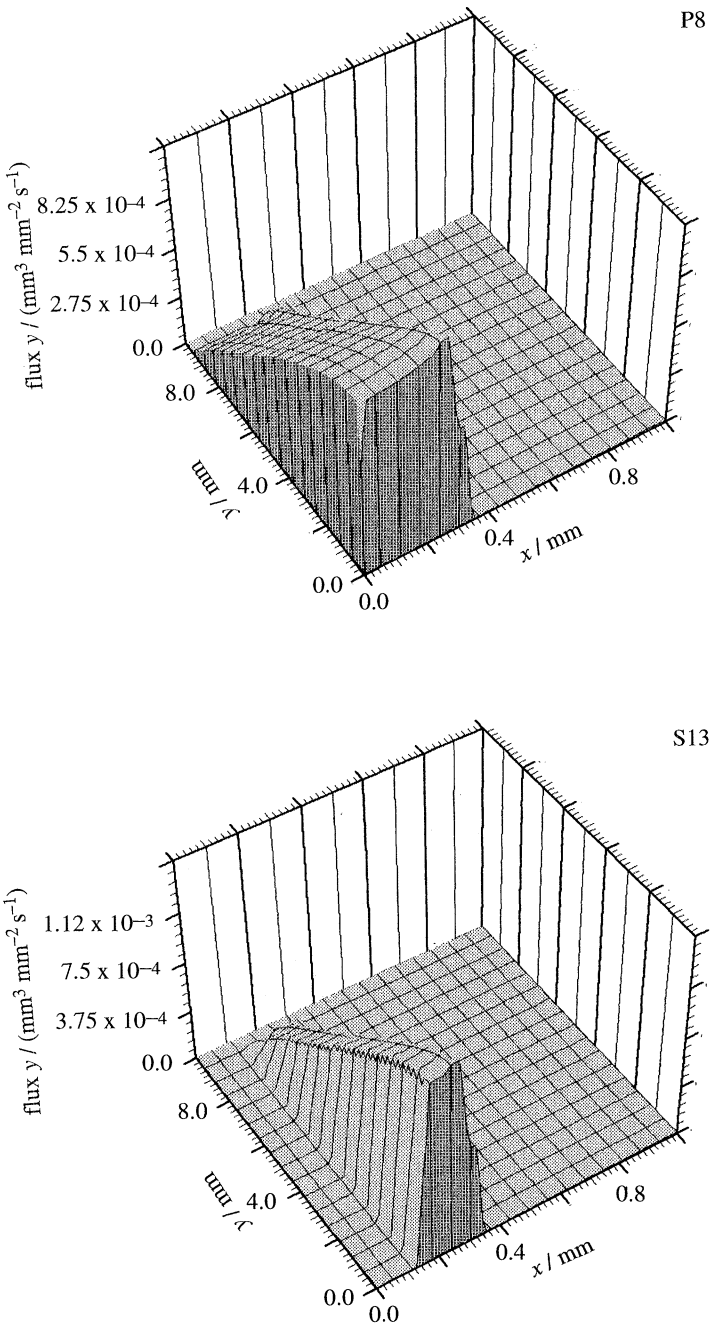

Figure 6. Three-dimensional representation of the vertical component of fluid flow velocity against spatial coordinates for structures P8 and S13 (at the steady state).

observed in the case of the siphonostelic structure S13. At early times, an inflow from the pith into the stele occurs (the flow vectors located at the left boundary are caused by graphical problems: the horizontally oriented vectors do not fit within the outlines of the structure). The flow from pith to stele decreases with time until it has ceased at the steady state condition. This means, that the stele takes up water from the pith during non-stationarity.

(*c*) *Temporal development of difference between inflow and outflow*

The results presented so far can also be illustrated by the temporal course of difference between basal inflow and transpiration. At steady state both are in balance. The system is losing water as long as it is not in the steady state. The volume of inflow into a structure at a discrete time was calculated by Simpson integration of the vertical flow velocities occurring at the bottom nodes. This gives the total volume of fluid flowing into the structure at a certain time. The transpiration rate is constant and was defined as 100%. The inflow was related to this value (Inflow_t = total $\text{inflow}_t \times \text{outflow}^{-1} \times 100$). Figure 9 shows the corresponding values for the structures P4, S14, P8 and S13 plotted against time. Again, the structures with identical *DX* show an almost identical behaviour.

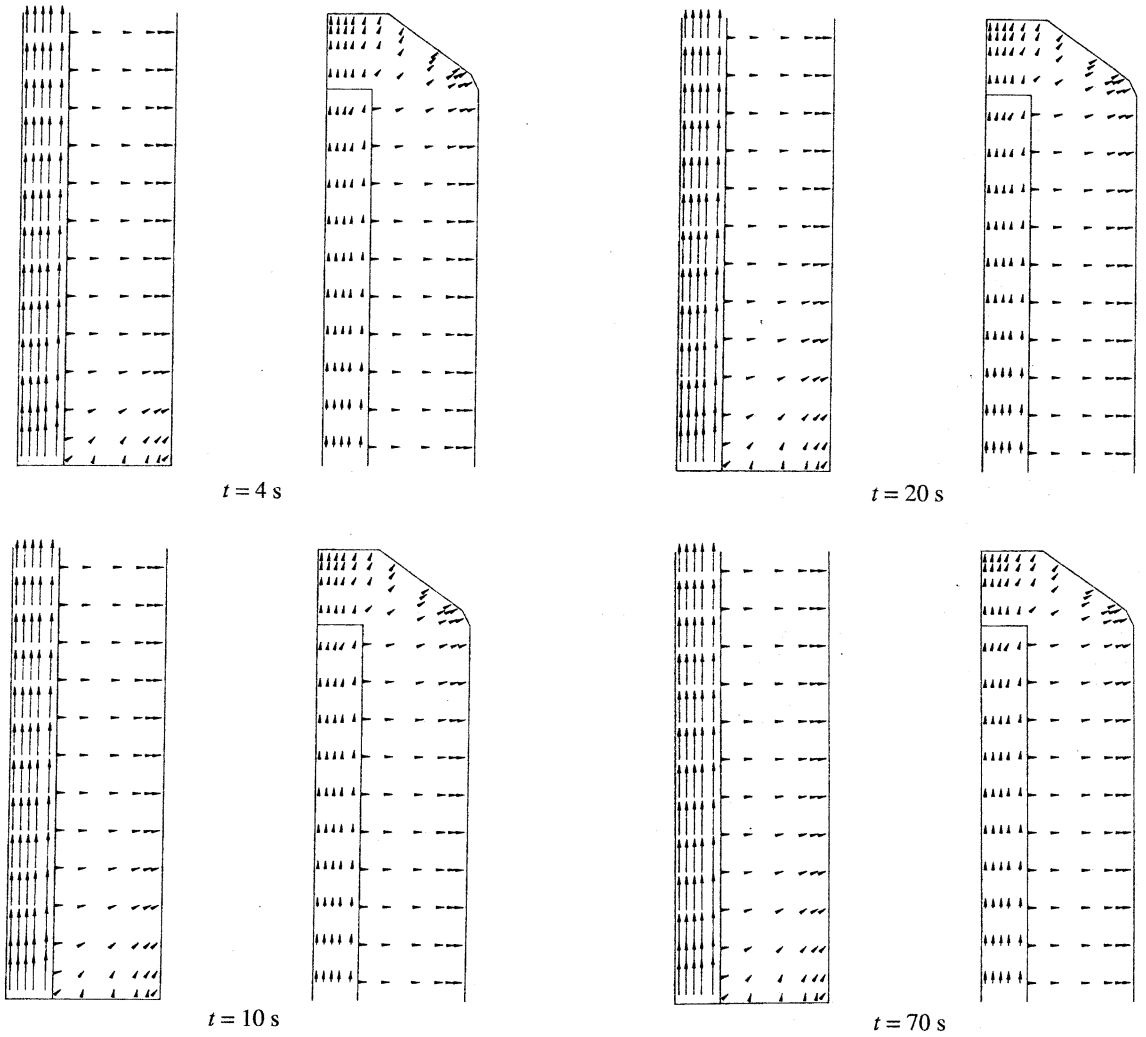

Figure 7. Fluid flows occurring in structure P8 at discrete times. The flows are represented as vector field (see text).

5. DISCUSSION

The topic of the simulations was to reveal how much protostele and siphonostele differ with regard to their water transport capabilities in order to yield functional interpretations of the early diversity of stelar constructions. The calculations brought several results concerning the hydrodynamic behaviour and efficiency of protostele and siphonostele. The time span required to reach the steady state, T_{stat}, was shown to depend not only on the relative amount of conducting tissue, but also on the distance between xylem and transpiring surface and is therefore also a subject of the architectonical arrangement of the conduits. T_{stat} has to be regarded as a parameter of water transport efficiency, because the longer this time period the more fluid loss occurs and it indicates therefore the reaction time of the system when transpiration starts or varies. A long parenchymatous path, which has to be passed by the water flow, prolongs the reaction time of the system. Furthermore, a high parenchymatous path length means a corresponding high pressure gradient extending over this path due to the low permeability of parenchyma. It is advantageous for a plant to keep the thickness of parenchyma between water sources and sinks small, because a short period of fluid loss and a lower pressure gradient mean less stress for the living tissue.

When plant size increases, then the path length between conduits and surface also increases given that the original protostele persists. Maintaining a small distance between xylem and transpiring surface could be achieved by enlarging the entire protostele, but this would result in an over-supply of the axis, because in this case the conducting portion as a fraction of the total axis would grow when cross-sectional area increases. As a consequence, the total volume of the stele can be diminished by abandoning the structure of a massive central strand. The actinostele evolved following this strategy. The xylem protuberances of the actinostele represent local diminishments of the parenchymatous layer between xylem and surface without enlargement of the entire stele. In principle, an actinostele represents a protostele with the surplus part of the xylem being removed. Another strategy is the suppression of unnecessary portions of the xylem in the central region of the stele. This results in the development of the siphonostele with a central pith. Arrangement of the conduits as siphonostele provides additional water storage. This was shown by the resulting fluid flows running from pith to stele during the non-steady phase or, in general, during a phase of

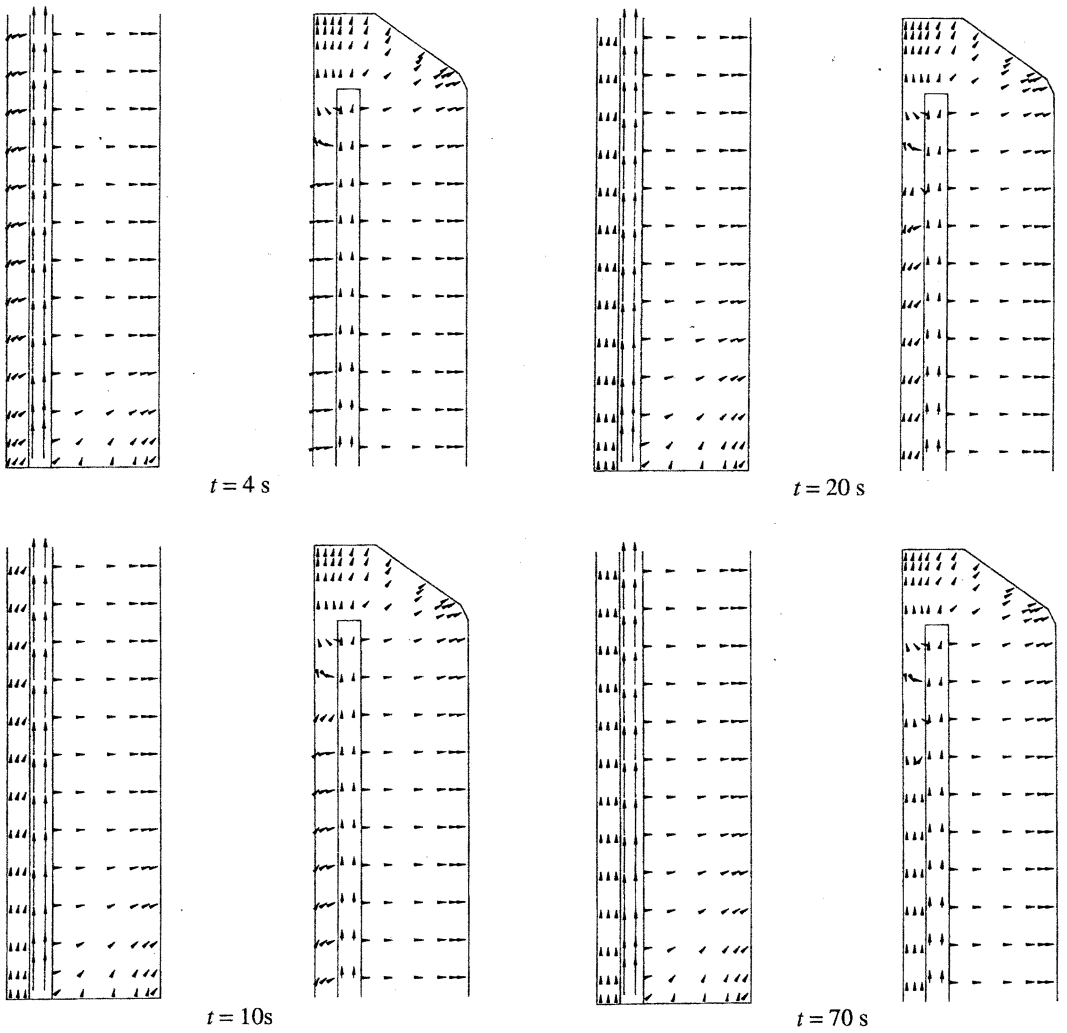

Figure 8. Fluid flows occurring in structure S13 at discrete times. The flows are represented as vector field (see text).

suboptimal water supply. If the inner xylem region of a protostele does not contribute to the water transport efficiency, then a siphonostele derived from it may behave hydrodynamically almost identically, as was demonstrated by the corresponding fluid pressure fields.

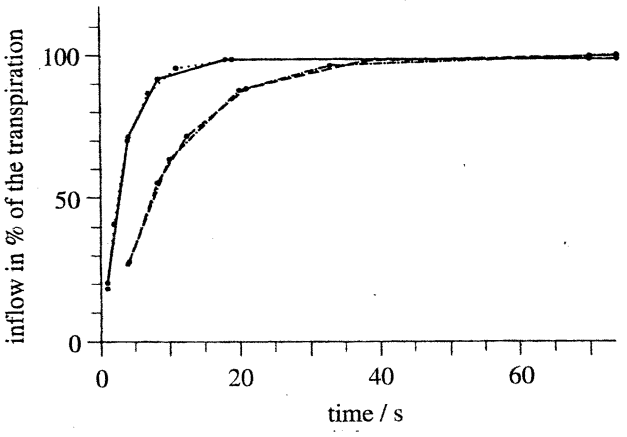

Figure 9. Temporal development of the inflow expressed as percentage values of the outflow, represented for structures P4 (solid line), P8 (dashed line), S13 (dot-dashed line) and S14 (dottped line). At T_{stat}, the inflow amounts 100% of the outflow.

The reduction of the xylem does not necessarily imply higher gradients of fluid pressure in the whole structure when the transpiration is maintained. The lower conducting area is compensated by higher fluid velocities in the conducting layer, as was shown by the longitudinal component of fluid velocity which was correspondingly higher in a siphonostele than in the protostele with equal distance from the surface. This means, that the increase of the fluid pressure gradient which is required to generate this higher fluid velocity concerns mainly the stele. A siphonostele is disadvantageous, however, because cortex and pith are separated by the hollow xylem cylinder. Lateral assimilate transport is severely restricted. A dissection of the cylinder permits connection between the regions of living tissues and offers the possibility of positioning the conducting units optimally. It could be assumed, that because of this effect a siphonostele is rarely expressed in plants. A usual stelar arrangement in ferns, for example, is the dictyostele which is a siphonostele perforated by numerous leaf traces. This construction is changed into a siphonostele, when the development of the leaf primordia is repressed, as was found by Ma & Steeves (1992). Thus, the vascular construction in a stem is governed by many factors and details of ontogenetic processes are complex at the level of higher plants.

The polystele, a stele composed of subunits, can also be considered in the context of water transport, because a number of discrete bundles can be distributed optimally over the entire cross-sectional area of the stem. In the case of high developed plant axes with secondary growth, however, the mechanical aspect of wood and its sclerenchymatic elements becomes more important, as the force of gravity increases with height of the structure. The stem of a tree has to function as a solid mechanical system which elevates the assimilating crown as high as possible (Mosbrugger 1990). The term stele, however, is no longer valid for such plant constructions, as was mentioned above (Beck *et al.* 1982).

As a whole, the results offer a causal explanation of early stelar evolution based on water transport demands. Enlarging the plant axis requires shifting of conduits to peripheral regions in order to optimize the arrangement of conducting tissue according to hydrodynamic requirements, an effect which was also supposed by Carlquist (1975). These relationships were very important in early land plants, as photosynthesis and transpiration took place mainly in the stem. Leaves, if they existed, played a minor role and an optimal supply of the stem was therefore essential. Moreover, water supply of the stem was also a mechanical factor, because the stability of early land plants was based mainly on the turgor of the tissue. Owing to these relationships, the enlargement of a primary plant axis effects generally the deviation of the stele from a protostelar construction. The results strongly support the view that a functional interpretation of stelar evolution must also take problems of water transport into account.

This work was supported by the Deutsche Forschungsgemeinschaft (SFB 230) and by a grant from the University of Bonn (Graduiertenförderungsgesetz Nordrhein-Westfalen) to A.R.

REFERENCES

Altman, P.L. & Dittmer, D.S. (eds) 1973 *Biology data book*, 2nd edn, vol. II. Bethesda: Federation of American Societies for Experimental Biology.

Bear, J. 1979 *Hydraulics of groundwater*. New York: Elsevier.

Beck, C.B., Schmid, R. & Rothwell, G.W. 1982 Stelar morphology and the primary vascular system of seed plants. *Bot. Rev.* **48**(4), 691–815.

Bierhorst, D.W. 1971 *Morphology of vascular plants*. New York: Macmillan.

Bold, H.C., Alexopoulos, C.J. & Delevoryas, T. 1980 *Morphology of plants and fungi*, 4th edn. New York, Cambridge, London: Harper and Row.

Bower, F.O. 1908 *The origin of the land flora*. London: MacMillan.

Bower, F.O. 1935 *Primitive land plants*. London: MacMillan.

Burström, H.G., Uhrström, I. & Olausson, B. 1970 Influence of auxin on Young's modulus in stems and roots of *Pisum* and the theory of changing the modulus in tissues. *Physiol. Pl.* **23**, 1223–1233.

Carlquist, S. 1975 *Ecological strategies of xylem evolution*. Berkeley, Los Angeles, London: University of California Press.

Chappell, T.W. & Hamann, D.D. 1968 Poisson's ratio and Young's modulus for apple flesh under compressive loading. *Trans. Am. Soc. agric. Engin.* **11**, 608–610.

Edwards, D. & Fanning, U. 1985 The microfossil record of early land plants: advances in understanding of early terrestrialization. *Phil. Trans. R. Soc. Lond.* B **309**, 147–166.

Grün, G.-U., Wallner, H. & Neugebauer, H.J. 1989 Porous rock deformation and fluid flow—numerical FE-simulation of the coupled system. *Geologische Rundschau* **78**(1), 171–182.

Jeronimidis, G. 1980 Wood—one of nature's challenging composites. In *The mechanical properties of biological materials* (34th Symposium of the Society for Experimental Biology) (ed. J. F. V. Vincent & J. D. Currey), pp. 169–182. Cambridge University Press.

Ma, Y. & Steevens, T.A. 1992 Auxin effects on vascular differentiation in ostrich fern. *Ann. Bot.* **70**, 277–282.

Molz, F.J. & Boyer, J.S. 1978 Growth-induced water potentials in plant cells and tissues. *Pl. Physiol.* **62**, 423–429.

Mosbrugger, V. 1990 The tree habit in land plants. (*Lect. Notes Earth Sci.* **28**). Heidelberg, Berlin, New York: Springer Verlag.

Niklas, K.J. 1984 Size-related changes in the primary xylem anatomy of some early tracheophytes. *Paleobiology* **10**(4), 487–506.

Niklas, K.J. 1988 Dependency of the tensile modulus on transverse dimensions, water potential, and cell number of pith parenchyma. *Am. J. Bot.* **75**(9), 1286–1292.

Niklas, K.J. 1992 *Plant biomechanics. An engineering approach to plant form and function*. Chicago, London: University of Chicago Press.

Raven, J.A. 1984 Physiological correlates of the morphology of early vascular plants. *Bot. J. Linn. Soc.* **88**, 105–126.

Roth, A., Mosbrugger, V. & Neugebauer, H.J. 1994 Efficiency and evolution of water transport systems in higher plants: a modelling approach. I. The earliest land plants. *Phil. Trans. R. Soc. Lond.* B **345**, 137–152.

Speck, T. 1991 Biophysikalische Methoden in der Paläobotanik: Möglichkeiten Problematik. *Ber. Naturf. Ges. Freiburg i. Br.* **79**, 99–131.

Speck, T. & Vogellehner, D. 1988 Biophysical examinations of the bending stability of various stele types and the upright axes of early 'vascular' land plants. *Bot. Act.* **191**, 262–268.

Stewart, W.N. & Rothwell, G.W. 1993 *Paleobotany and the evolution of plants*, 2nd edn. Cambridge University Press.

Vincent, J.F.V. & Jeronimidis, G. 1991 The mechanical design of fossil plants. In *Biomechanics in evolution* (ed. J. M. V. Rayner & R. J. Wootton), pp. 21–36. Cambridge University Press.

Vincent, J.F.V. 1982 The mechanical design of grass. *J. Mater. Sci.* **17**, 856–860.

Wainwright, S.A., Biggs, W.D., Currey, J.D. & Gosline, J.M. 1976 *Mechanical design in organisms*. London: Edward Arnold.

Wallner, H. 1990 Finite Elemente Simulation von Fluidbewegungen in einem deformierbaren poroelastischen Medium mit druckabhängiger Permeabilität. Ph.D. thesis, TH Clausthal.

Weast, R.C. & Astle, M.J. (eds) 1983 *CRC handbook of chemistry and physics*. Boca Raton, Florida: CRC Press.

Zienkiewicz, O.L. & Taylor, R.L. 1989 The finite element method, 4th edn, vol. 1. London, New York: McGraw-Hill.

Zimmermann, W. 1959 *Die Phylogenie der Pflanzen*. Stuttgart: Gustav Fischer Verlag.

Received 18 October 1993; accepted 19 January 1994

PHILOSOPHICAL TRANSACTIONS OF THE ROYAL SOCIETY B BIOLOGICAL SCIENCES